ADCONIP 2014 Hiroshima

Small Unmanned Aerial Vehicle with Variable Geometry Delta Wing

Koji Nakashima [1], Kazuo Okabe [1], Yasutaka Ohsima[2], Shuichi Tajima[2] and Makoto Kumon[2]

***Abstract*— The kiteplane that is considered in this paper has stable attitude dynamics and flies slowly owing to its large main wing, which is suitable for ground observation. The rudder locates behind the propeller and its aerodynamic response is effected by the air flow induced by the thrust. This coupling interference makes the control of the kiteplane difficult, especially when the thrust is largely deviated from the nominal situation. The paper proposes a variable geometry delta wing mechanism for the kiteplane. This is intended to remove the coupling effect among the thrust and control surfaces since the air flow around the main wing is almost constant during the all flight conditions. The paper also shows experimental results to validate the proposed method.**

I. INTRODUCTION

Rescue activities and surveillance missions in dangerous areas, such as those affected by natural disasters, are important in order to save victims and obtain important data. Those areas are not always easily accessible by ordinary means since the infrastructure can be severely damaged. Therefore, unmanned aerial vehicles (UAVs) are expected to be used because they are able to be operated remotely, and they have been studied actively (for example, [1], [2]).

In this paper, a lightweight fixed-wing UAV with a large main wing that realizes a slow flight speed is considered. This UAV is named a kiteplane because its main wing is made of cloth and has a delta triangle shape like a kite, as shown in Fig. 1.

(a) Conventional (b) Proposed

Fig. 1. Kiteplane

Originally, the kiteplane was developed to have three control surfaces, rudder, elevator and a pair of ailerons so that they could control yaw, pitch and roll motion (Fig.1 (a)). For the original kiteplane, Nagata [3] proposed PID control because of its simple dynamics, and the author [4] proposed a fuzzy-logic based nonlinear flight controller for waypoint tracking. These methods use the position of the aircraft to control its flight path without considering the attitude due to its stable dynamics. The authors [5] also proposed a nonlinear control method of its attitude to realize path-following control.

Since both the aileron and the rudder are effective to control direction of flight, the original configuration was redundant. From this viewpoint, the pair of ailerons was removed in order to make the system simple, and only the rudder has been utilized to control the bearing. On the other hand, because of the fact that the rudder locates behind the propeller that generates thrust to push the airplane, the air flow around the rudder surface depends on the operating condition of the propeller. The controller proposed in [4] included a compensator for this effect under the assumption that the relationship between the thrust and the aerodynamic parameters of the rudder can be modeled by a static linear function, which worked properly for steady flight. Even with this compensation, it was not sufficient for the case when the rotation speed of the propeller was largely deviated from the nominal model. In order to overcome this difficulty, the present paper proposes to introduce variable geometry mechanism for the kiteplane to deform the shape of the main wing. The mechanism varies the ratio of the area of the left and the right half of the main wing so that the main wing itself can generate roll moment. Since the air flow around the main wing is almost constant during the flight even at take-off or landing, the control surface is expected to perform equally under various flight conditions. The main contribution of the present paper is to propose the variable geometry delta wing UAV and to evaluated the approach through real experiments.

The present paper is organized as follows: In the next section, the kiteplane with the variable geometry wing and its dynamics are briefly introduced. Then, the embedded control system is briefly shown in Sec. III. The main part of the paper to investigate the effectiveness of the proposed variable geometry wing is shown in Sec. IV, and then the conclusions follow in Sec. V.

II. KITEPLANE WITH VARIABLE GEOMETRY DELTA WING

A. Kiteplane

A kiteplane is a UAV that has a kite-like main wing in the shape of a delta, as shown in Fig. 1. The main wing is light and flexible because it is made of cloth, and the UAV is capable of carrying a large payload. The wing's flexibility provides safety and robustness if it crashes into the ground. The center of mass is located under the main wing. The

[1]Koji Nakashima and Kazuo Okabe are with Skyremote Inc., 2-3-10, Mukae-machi, Chuo-ku, Kumamoto, 860-0817, Japan

[2]Makoto Kumon, Yasutaka Ohisima and Shuichi Tajima are with Graduate School of Science and Technology, Kumamoto University, 2-39-1, Kurokami, Chuo-ku, Kumamoto, 860-8555, Japan, kumon@gpo.kumamoto-u.ac.jp

kiteplane's length, wingspan, and height are 1160 mm, 900 mm, and 2040 mm, respectively, and it weighs approximately 4.5 kg.

The kiteplane has three control surfaces: the variable geometry main wing, the elevator, and the rudder, and they are actuated by servomotors. The propeller that generates the thrust required to fly is driven by a brushless motor, and its rotational speed is controlled by a speed controller.

A global positioning system (GPS) is installed to measure the delta wing's position, and a three-dimensional accelerometer, a three-dimensional rate gyro, and a three-dimensional magnetometer are also installed to estimate the attitude of the aircraft.

Denote aerodynamic forces effecting to the mainwing (left half and right half), elevator, rudder and thrust as $\boldsymbol{f_{m,l}}$, $\boldsymbol{f_{m,r}}$, $\boldsymbol{f_e}$, $\boldsymbol{f_r}$ and $\boldsymbol{T}$ respectively.

Considering the UAV as a rigid body, the motion equation with respect to the center of mass can be given as follows:

$$m\frac{d^2}{dt^2}\begin{bmatrix} x_I & y_I & z_I \end{bmatrix}^{\mathrm{T}} = \boldsymbol{f_I}, \tag{1}$$

$$\boldsymbol{I_B}\frac{d}{dt}\boldsymbol{\omega_B} + \boldsymbol{\omega_B} \times \boldsymbol{I_B}\boldsymbol{\omega_B} = \boldsymbol{n_B}, \tag{2}$$

where

$$\begin{aligned} \tilde{\boldsymbol{f_I}} &= \boldsymbol{q} \odot \tilde{\boldsymbol{f_B}} \odot \boldsymbol{q}^* \\ &= \boldsymbol{q} \odot \left(\tilde{\boldsymbol{f_{m,l}}} + \tilde{\boldsymbol{f_{m,r}}} + \tilde{\boldsymbol{f_e}} + \tilde{\boldsymbol{f_r}} + \tilde{\boldsymbol{T}} \right) \odot \boldsymbol{q}^* \\ \boldsymbol{n_B} &= \boldsymbol{l_{m,l}} \times \boldsymbol{f_{m,l}} + \boldsymbol{l_{m,r}} \times \boldsymbol{f_{m,r}} + \boldsymbol{l_e} \times \boldsymbol{f_e} \\ &\quad + \boldsymbol{l_r} \times \boldsymbol{f_r} + \boldsymbol{l_T} \times \boldsymbol{T}, \end{aligned}$$

and the quantity represented as $\tilde{\boldsymbol{x}}$ implies quaternion with the vector $\boldsymbol{x}$ for its imaginary part (*i.e.,* $\tilde{\boldsymbol{x}} = \left[0, \boldsymbol{x}^T\right]^T$).

Here, x_I, y_I, and z_I indicate the position of the body, and $\boldsymbol{\omega_B}$ represents the angular velocity. The attitude is represented by a quaternion $\boldsymbol{q}$, and $\odot$ represents the multiplication of quaternions. $\boldsymbol{f_I}$ and $\boldsymbol{f_B}$ represent the forces acting on the center of mass with respect to the body frame and the inertial frame, respectively, and $\boldsymbol{n_B}$ denotes the torque on the body. The translation between $\boldsymbol{f_I}$ and $\boldsymbol{f_B}$ can be given by using a quaternion as shown above, and * shows the conjugate operation of the quaternion. m and $\boldsymbol{I_B}$ represent the mass of the body and the inertial matrix, respectively. $\boldsymbol{l_{m,l}}$, $\boldsymbol{l_{m,r}}$, $\boldsymbol{l_e}$, $\boldsymbol{l_r}$, and $\boldsymbol{l_T}$ represent the position of the aerodynamic forces acting on the wings. Further details of the quaternion operations can be found in [6]. The attitude is represented by the quaternion, and its dynamics are given as follows:

$$\frac{d}{dt}\boldsymbol{q} = \frac{1}{2}\tilde{\boldsymbol{\omega_I}} \odot \boldsymbol{q} = \frac{1}{2}\boldsymbol{q} \odot \tilde{\boldsymbol{\omega_B}} \tag{3}$$

Let the state of the system be represented by $(x_I, y_I, z_I, \frac{d}{dt}x_I, \frac{d}{dt}y_I, \frac{d}{dt}z_I, \boldsymbol{q}, \boldsymbol{\omega_B})$. Recalling the fact that $\boldsymbol{f_B}$ and $\boldsymbol{n_B}$ can be computed if the state and control inputs are given, the evolution of the system can be obtained by the dynamics (1), (2), and (3).

Detailed dynamics of the UAV can be found in [5], [4], but the proposed variable geometry main wing is shown in the next subsection in detail.

B. Variable Geometry Wing

As it has been mentioned in the previous sections, the interference between the thrust, or the rotation speed of the propeller, and the rudder could make it difficult for the autonomous controller to maintain the desired attitude when the thrust becomes largely deviated from the nominal condition. This is the physical nature of the UAV itself, and it is efficient to develop a simple system the attenuate this significant interference.

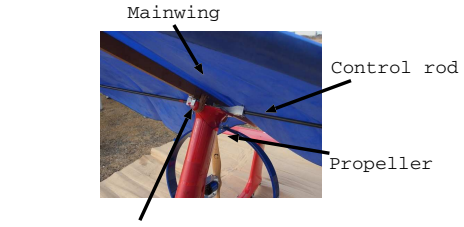

(a) Photo of the mechanism

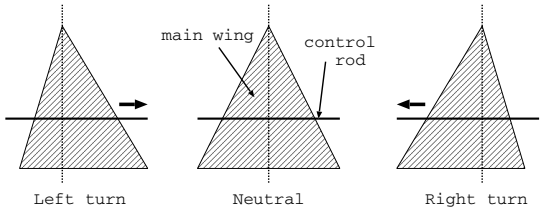

(b) Control action of the mechanism

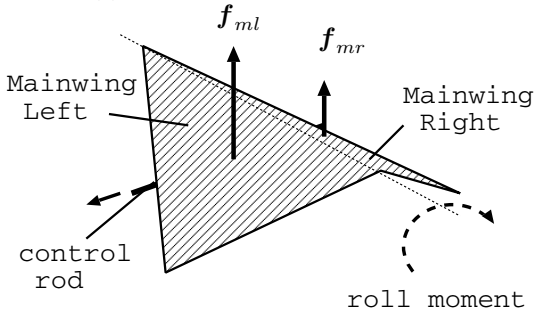

(c) Aerodynamic forces effecting to the main wing

Fig. 2. Variable geometry wing mechanism

To this end, the present paper proposes to introduce variable geometry mechanism for the main wing. This is possible since the main wing of the kiteplane is made of cloth and it is easy to deform its shape by moving its frames. A servo motor is installed at the center of the main body that supports the main wing, and the motor moves the rod to left or right according to the control command. As this rod moves, areas of the left and the right half of the main wing varies.

A simple aerodynamic model of the main wing can be written as

$$\begin{aligned} \left|\boldsymbol{f}_{m,l}\right| &= \frac{1}{2}S_{m,l}\rho V^2 C_{L,m} \\ \left|\boldsymbol{f}_{m,r}\right| &= \frac{1}{2}S_{m,r}\rho V^2 C_{L,m}, \end{aligned}$$

where $\boldsymbol{f}_{m,l}$, $\boldsymbol{f}_{m,r}$, $S_{m,l}$, $S_{m,r}$, ρ, V and $C_{L,m}$ represent aerodynamic force of the left half and that of the right half, areas of the left half and the right half, air density, speed of the air flow around the main wing and aerodynamic coefficient respectively. Denote the deviation of the control rod from the center as u_m, and assume that the magnitude of u_m is small. Then, areas of the left and the right half of the main wing can be modeled as

$$S_{m,l} = S_m + \alpha u_m, \quad S_{m,r} = S_m - \alpha u_m, \tag{4}$$

where S_m and α represent the neutral area and a constant coefficient. From (4) and the structure of the control surfaces attached to the body, the roll moment, or the x component of the moment $\boldsymbol{n_B}$ in (2), can be written as

$$n_{B,x} \approx \beta u_m + \gamma,$$

where β and γ represent constant parameters. For example, the magnitude of $\boldsymbol{f_{m,l}}$ becomes larger than that of $\boldsymbol{f_{m,r}}$ when the control rod is moved to the left, which generates the clockwise roll moment as shown in Fig.2(b) and (c).

As the UAV flies, the existence of the lower bound of the airspeed V can be guaranteed, and the area of the main wing is sufficiently large to work as a control surface. Therefore, it can be guaranteed that the moment generated by $\boldsymbol{f_{m,l}}$ and $\boldsymbol{f_{m,r}}$ effects all the time through the flight, which is different from the case of the rudder.

III. CONTROL SYSTEM

The embedded control system developed in [7] is briefly shown in this section.

The control module (Fig.3) consists of a ARM Cortex-3 microprocessor and a sensor module that has three rate-gyros, three accelerometer and three magnetometer with uBlox GPS module. The microprocessor receives the servo control signals from the operator through the radio transmitter, and it modulates those signals according to the programmed control laws such as proposed in [5]. For the case of emergency, the microprocessor can be turned off by the radio signal from the ground station, and all servo motors can be controlled manually.

The microcontroller is also programmed to estimate the attitude of the UAV based on the quaternion computed from the rate gyros and the quaternion by QUEST[8] using the information from the accelerometer and the magnetometer.

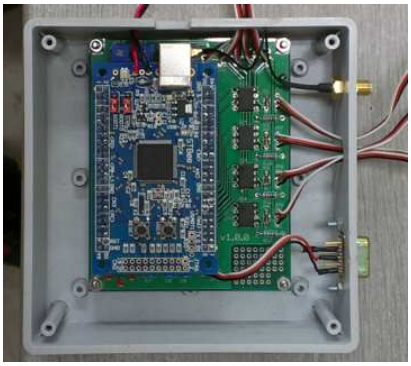

Fig. 3. Embedded control module

Because the main contribution of this paper is to propose the variable geometry wing mechanism for the kiteplane, only a simple controller to keep the attitude stable is installed. The angular velocity $\boldsymbol{\omega_B}$ can be measured by the rate gyros, and the following control law was implemented:

$$\begin{bmatrix} u_m \\ u_e \\ u_r \end{bmatrix} = -\boldsymbol{K}\boldsymbol{\omega_B} + \boldsymbol{u}, \tag{5}$$

where u_m, u_e, u_r, $\boldsymbol{K}$ and $\boldsymbol{u}$ represent commands for main-wing deformation, elevator, rudder, a constant gain matrix and the command by the operator.

IV. EXPERIMENT

For the first experiment, flight tests with the kiteplane were conducted to evaluate the proposed mechanism by comparing effect of the rudder and the aileron. Then, the simple feedback law (5) was introduced to test whether the flight dynamics could be stabilized.

A. Setup

The UAV was launched manually to a sufficiently high altitude. For the first experiment, it was commanded to turn by

1-a) the variable geometry wing with the propeller running,

1-b) the variable geometry wing with the propeller stalled,

2-a) rudder with the propeller running,

2-b) rudder with the propeller stalled,

in order to clarify that the proposed mechanism is less affected by the state of the thrust. Feedback law (5) was turned off in this experiment so to verify the dynamics of the kiteplane itself.

For the second experiment, the UAV was operated to turn manually, and then the operator put the input $\boldsymbol{u}$ in (5) at the neutral state so that the feedback law governs the dynamics of the system. The feedback law gain in (5) was selected as $\boldsymbol{K} = 45\boldsymbol{I}_3$ where $\boldsymbol{I}_3$ shows a 3 by 3 identity matrix.

The kiteplane used in this experiment had a mainwing of XXXm wide, and $S_m \approx 1.0[\mathrm{m}^2]$. The rod to control could travel about ± 12[mm] that is connected to the control action αu_m in (4).

B. Result

1) Comparison of Variable Geometry Wing and Rudder: The flight was longer than 250 seconds, and its flight path is shown in Fig.4. During the flight, four cases explained above were tested and they are shown in Fig.5 and 6 for 1-a and 2-a cases, and in Fig.7 and 8 for 1-b and 2-b cases. Fig.5 and 7 show control commands of the variable geometry wing, the rudder and the thrust, and Fig.6 and 8 show corresponding flight paths starting at red crosses and ending at green circles (top figures), and the magnitude of angular velocity $\boldsymbol{\omega}_B$ (bottom).

As the thrust command was kept large in Fig.5, the propeller was running for the duration from 900 to 920

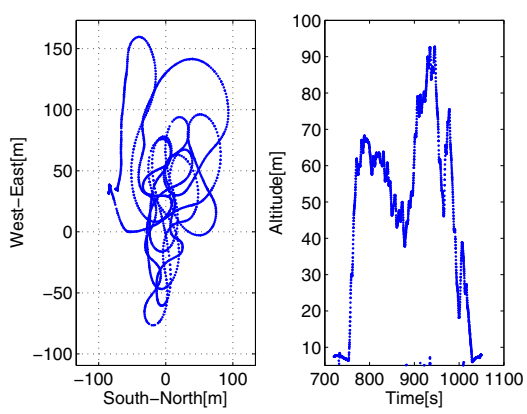

Fig. 4. Flight path

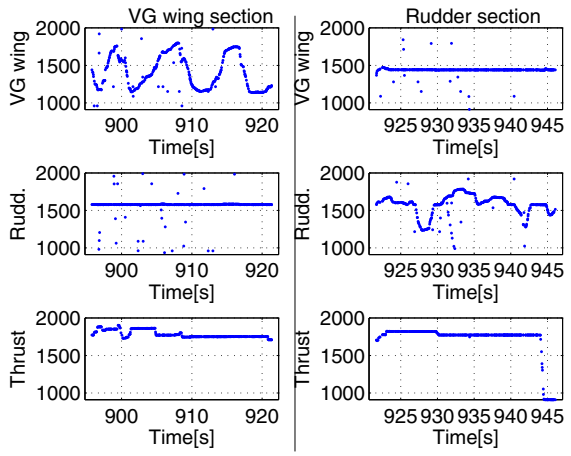

Fig. 5. Control commands (propeller run)

Control commands of the variable geometry wing, the rudder and the thrust (propeller rotation) are shown. The left three figures show those values when only the variable geometry wing was activated while the rudder was fixed, and the right three show the commands when the rudder was activated instead.

seconds when the variable geometry wing was activated while the rudder was kept constant (1-a), and for the duration from 925 to 940 seconds when the rudder was activated instead (2-a). Fig.6 shows that the UAV turned according to the both command of the variable geometry wing and the rudder.

On the other hand, Fig.7 shows that the thrust command was kept small, which implies that the propeller was stalled, for the duration from 945 to 975 seconds (1-b) and that from 978 to 992 seconds (2-b). Note that the rudder command in Fig.7 was given as the maximum and the minimum values for more than 10 seconds, which means the operator tried to turn the UAV drastically compared to the case when the propeller was running. From corresponding results shown in Fig.8, the UAV was able to respond to the commands to turn for both cases, but the response for the rudder case (2-

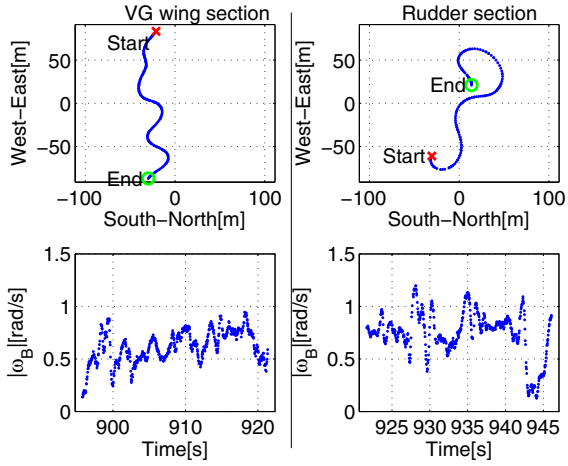

Fig. 6. Response of the kiteplane (propeller run)

Flight path (top), response of the magnitude of the angular velocity $|\boldsymbol{\omega}_B|$ (bottom) are shown. As in Fig.5, the left figures show them when the variable geometry wing was activated, and the right ones show when the rudder was on instead. In the top figure, red cross and green circle show positions of the UAV at the beginning and the end of the period.

b) was not as sensitive as the propeller was running (1-b). This can be quantified from the magnitude of the angular velocity shown at the bottom figures of Fig.6 and 8. The angular velocity of the case 2-b was half of that of 1-b even with the maximum command signal, although there was not clear difference between 1-a and 2-a cases.

2) Stabilizing control: In the second experiment, the control law (5) was tested. The UAV was commanded to turn by the variable geometry wing, and then the command by the operator was kept at the neutral value as shown in Fig.9. The responses are shown in Fig.10. Owing to the turn command by the operator at the beginning of the trial, the UAV turned left with a roll action ($\omega_{B,x} < 0$ represents the roll to left). Once the operator removed his command (at 797 sec.), the UAV came back to the straight flight, and all angular velocities diminished. This validates that the straight flight state of the UAV was stable under the control law of (5).

V. CONCLUSION

The present paper proposes a variable geometry delta wing mechanism for the kiteplane in order to provide stable control actions even when the propeller is stopped. Experiment with the developed platform was conducted, and the comparison between the turn with the rudder, and that with the proposed main wing validates the approach.

Since the mainwing is made of cloth, it can deform largely if the control rod travels significantly large, which may break the assumption of (4). Further investigation of the deformation of the mainwing is still necessary. Besides, path-following control as proposed in [5] with the developed system is one of future works.

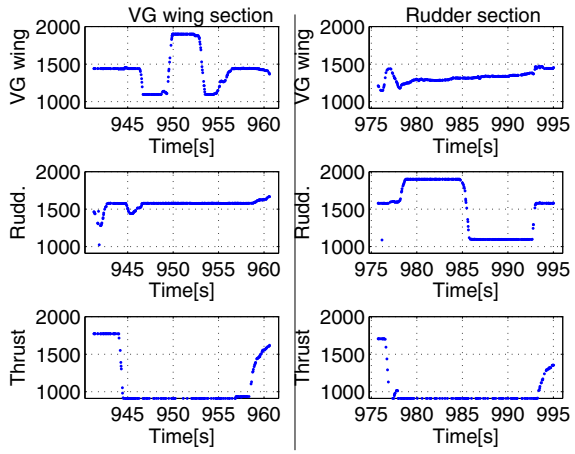

Fig. 7. Control commands (propeller stop)

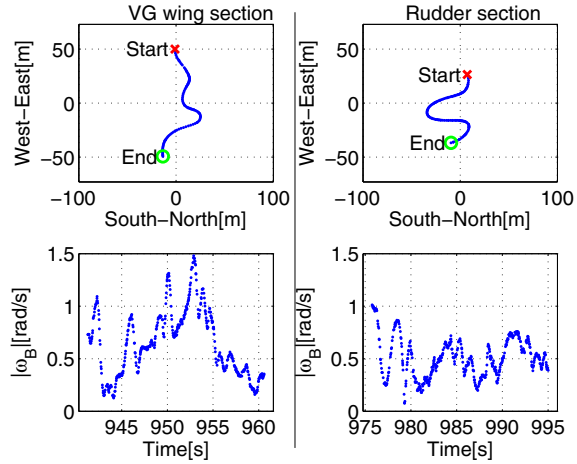

Fig. 8. Response of the kiteplane (propeller stop)

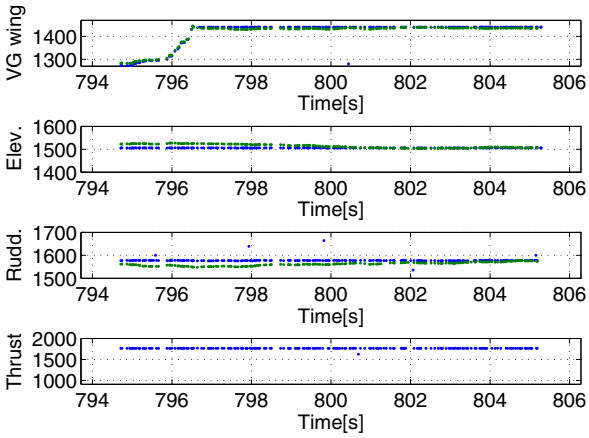

Fig. 9. Control cmd with the stabilization control

Blue dots shows the command by the operator ($\boldsymbol{u}$ in (5)), and green dots shows the actual commands u_m, u_e and u_r. Since a control law for the thrust command is not considered in this paper, the thrust command by the operator is commanded.

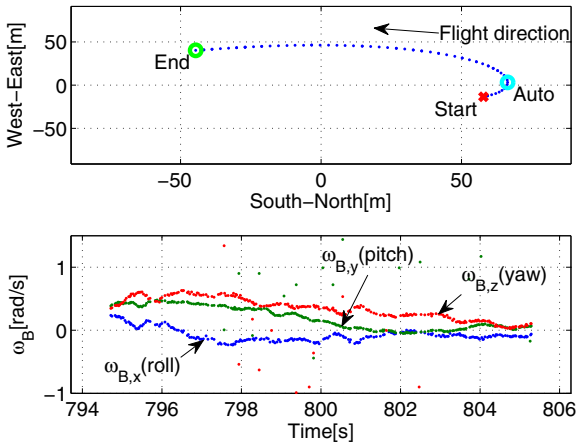

Fig. 10. Response of the kiteplane with the stabilization control

Top figure shows the flight path corresponding to Fig.9 where red cross and green circle show the beginning and the end of the section. Light blue circle shows when the operator stopped his operation ($t = 797$ s).

ACKNOWLEDGEMENT

This work was partially supported by JSPS KAKENHI Grant Number 24220006.

REFERENCES

[1] T. Mueller and J. D. DeLaurier, "An overview of micro air vehicle aerodynamics." *Progress in Astronautics and Aeronautics*, vol. 195, pp. 1–10, 2001.

[2] H. Chao, Y. Cao, and Y. Chen, "Autopilots for small unmanned aerial vehicles: a survey," *International Journal of Control, Automation and Systems*, vol. 8, no. 1, pp. 36–44, 2010.

[3] M. Nagata, M. Kumon, R. Kouzawa, I. Mizumoto, and Z. Iwai, "Automatic flight path control of small unmanned aircraft with delta-wing," in *Proc. of the Int. Conf. on Control, Automat. and Syst.*, Bangkok, Thailand, Aug. 2004, pp. 1383–1388.

[4] M. Kumon, Y. Udo, H. Michihira, M. Nagata, I. Mizumoto, and Z. Iwai, "Autopilot system for kiteplane," *IEEE/ASME Transactions on Mechatronics*, vol. 11, no. 5, pp. 615–624, oct 2006. [Online]. Available: http://ci.nii.ac.jp/naid/120002464294/

[5] S. Tajima, T. Akasaka, M. Kumon, and K. Okabe, "Guidance control of a small unmanned aerial vehicle with a delta wing," in *Proceedings of Australasian Conference on Robotics and Automation*, 2013.

[6] R. M. Murray, Z. Li, and S. S. Sastry, *A Mathematical Introduction to Robotic Manipluation*. CRC Press, 1994.

[7] S. Tajima, Y. Ohsima, M. Kumon, and H. Hata, "Development of small attitude estimation system for kite plane," in *Proceedings of the 14th System Integration Division of SICE*, 2013, pp. 357–359, (in Japanese).

[8] M. D. Shuster and S. D. Oh, "Three-axis attitude determination from vector observations," *Journal of Guidance, Control, and Dynamics*, vol. 4, no. 1, pp. 70–77, 1981.